Journal of Materials Science and Chemical Engineering, 2022, 10, 63-69
https://www.scirp.org/journal/msce
ISSN Online: 2327-6053
ISSN Print: 2327-6045

3D Bio-Printed Bone Scaffolds Incorporated with Natural Antibacterial Compounds

Zhuo Zhang[1*], Yiqi Yang[2], Hongbo Zhang[1#], Shengbing Yang[2], Ruixue Yin[1], Wenjun Zhang[1]

[1]Complex and Intelligent Research Center, East China University of Science and Technology (ECUST), Shanghai, China
[2]Shanghai Key Laboratory of Orthopaedic Implants, Department of Orthopaedic Surgery, Shanghai Ninth People's Hospital, Shanghai Jiao Tong University School of Medicine, Shanghai, China
Email: #hbzhang@ecust.edu.cn

How to cite this paper: Zhang, Z., Yang, Y.Q., Zhang, H.B., Yang, S.B., Yin, R.X. and Zhang, W.J. (2022) 3D Bio-Printed Bone Scaffolds Incorporated with Natural Antibacterial Compounds. *Journal of Materials Science and Chemical Engineering*, **10**, 63-69.
https://doi.org/10.4236/msce.2022.103005

Received: February 27, 2022
Accepted: March 27, 2022
Published: March 30, 2022

Abstract

3D Bioprinting plays an irreplaceable role in bone tissue engineering. Shellac and curcumin are two natural compounds that are widely used in the food and pharmaceutical sectors. In this study, a new composite scaffold with good biocompatibility and antibacterial ability was manufactured by adding shellac and curcumin into the traditional bone scaffold through low-temperature three-dimensional printing (LT-3DP), and its impact on the osteoimmune microenvironment was evaluated.

Keywords

Bone Tissue Engineering, 3D Printing Bone Scaffold, Antibacterial, Shellac, Curcumin

1. Introduction

3D printing technology is developing rapidly in the medical field. LT-3DP plays a unique role in the manufacture of bone scaffolds due to its characteristics of maintaining the biological activity and wide compatibility of materials [1] [2] [3]. β-Tricalcium phosphate (β-TCP) and nano-hydroxyapatite (nHA) are bioceramics commonly used for bone scaffolds due to their similar properties to natural bone and good biocompatibility [4] [5]. However, such scaffolds are still lack of antibacterial function, which is crucial in bone implants [6] [7].

In this paper, to obtain a bone scaffold with both antibacterial and osteogenic properties, natural compounds of shellac and curcumin were added to the traditional 3D bio-printed bone scaffolds. The antimicrobial results indicate that the new scaffolds are better antimicrobial agents as compared to other groups, while

*First author.
#Corresponding author.

its biocompatibility was not significantly reduced. Furthermore, increased secretion of pro-inflammatory factors was not observed when the scaffold was cocultured with THP-1 cells. The composite scaffolds have broad applications.

2. Materials and Methods

2.1. Material Scaffold Fabrication

The basic components of bone scaffolds include β-TCP (DK Nano, China), HA (MACKLIN, China), and poly(ε-caprolactone) (PCL) (molecular weight = 65 kg/mol; Daigang, China). 0.6 g of PCL were dissolved in 5 mL of dichloromethane at 21˚C ± 1˚C. Then 1.8 g β-TCP and 0.6 g HA were added to the solution, together with 1.8 mL of absolute ethanol to control the viscosity of slurry. 30 mg shellac (Acid value 40 - 70 mg KOH/g; Rhawn, China) and 3 mg curcumin (MACKLIN, China) were dissolved in ethanol and added to slurry for printing.

The composite scaffold was manufactured using a 3D printer (3D Bioplotter; EnvisionTec, German). The diameter of the printing nozzle is 410 μm, and the printing speed is 4 - 6 mm/s. The printing speed and pressure were adjusted to continuously extrude lines with uniform thickness. The spacing of parallel lines is set to 0.8 mm, and the ambient temperature is 21˚C ± 1˚C. The scaffolds were printed on the slide and stored at −20˚C away from light after removal. The blank scaffolds contain PCL, β-TCP and HA, as group A. The scaffolds were named group B when mixed with shellac, and group C with shellac and curcumin. The manufacturing process and the morphology of the scaffolds are shown in **Figure 1**.

2.2. Characterization

2.2.1. Scanning Electron Microscope

The morphology of scaffold was observed by scanning electron microscope (SEM) (S-3400N; Hitachi Ltd., Japan). After freeze-drying for 24 hours, the sample was placed on the copper table and plated with a layer of gold (3 nm).

2.2.2. Fourier Transform Infrared Spectroscopy

The infrared spectra (FTIR) of scaffolds and materials were obtained using an

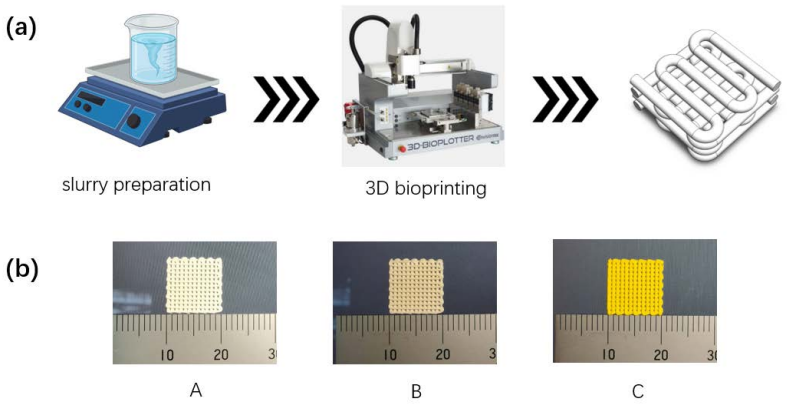

Figure 1. (a) Schematic diagram of scaffold preparation. (b) Morphology of different scaffolds.

FTIR spectrometer (6700; thermo Nicolet Corporation) and in attended total reflection (ATR) mode.

2.3. Antibacterial Properties Test

Staphylococcus aureus (S. aureus) was used to evaluate the antibacterial activity of the materials. 30% absolute ethanol and 70% saline were used as bacterial diluent. In order to dissolve lac and curcumin, the final concentration of shellac was 21 mg/mL, and that of curcumin was 2.1 mg/mL. After incubation at 37˚C for 24 h, the colony area was calculated by ImageJ. Three parallel experiments were carried out.

2.4. Biocompatibility Test

Different concentrations of shellac were dissolved in DMEM medium (containing 10% fetal bovine serum and 1% penicillin-streptomycin) at the concentration of 2 μg/mL, 1 μg/mL, 0.5 μg/mL, 0.25 μg/mL, 0.1 μg/mL and 0 μg/mL, respectively. Shellac was dissolved using dimethyl sulfoxide, the final concentration of which is 1%. C2C12 cells were cultured in 48 well plates with DMEM medium containing shellac at the concentration of 3×10^3 cells per well. The blank group used an ordinary medium. The Cell counting kit-8 (CCK-8) assay was performed using a CCK8 kit (kingmorn, China) following the manufacturers' protocol.

The absorbance of shellac solution was measured at the wavelength of 200 nm, the concentration standard curve of lac in the culture medium was fitted. The sample extract was prepared according to GBT 16,886.12. The absorbance value of shellac scaffold extract was measured, and the concentration was calculated according to the standard curve.

C2C12 cells in logarithmic growth phase were inoculated into 48 well plates at the concentration of 3×10^3 cells per well, and cultured with the extract of three groups of scaffolds respectively. The blank group was added with an ordinary medium. The live and dead staining images were obtained using Calcein-AM (CAM) and propidium iodide (PI) (Dojindo, China).

2.5. Cytokine Assay

THP-1 cells were used to test the immunomodulatory effect of the composite scaffold. After treated with PMA at the concentration of 100 ng/mL for 48 h, Thp-1 cells were added to a scaffold ($10 \times 10 \times 1$ mm^3) placed in a 24 well plate with the amount of 5×10^4 cells per well. The cell culture medium was collected and centrifuge at the speed of 2000 r/min for 20 min after 48 h. The supernatant was taken and the contents of TNF-*a*, IL-6 and L-10 were determined by ELISA kit (Mlbio, China). Three parallel experiments were carried out.

3. Results and Discussion

3.1. Characterization

SEM results of the scaffolds are shown in **Figure 2(a)**. The smooth part of the

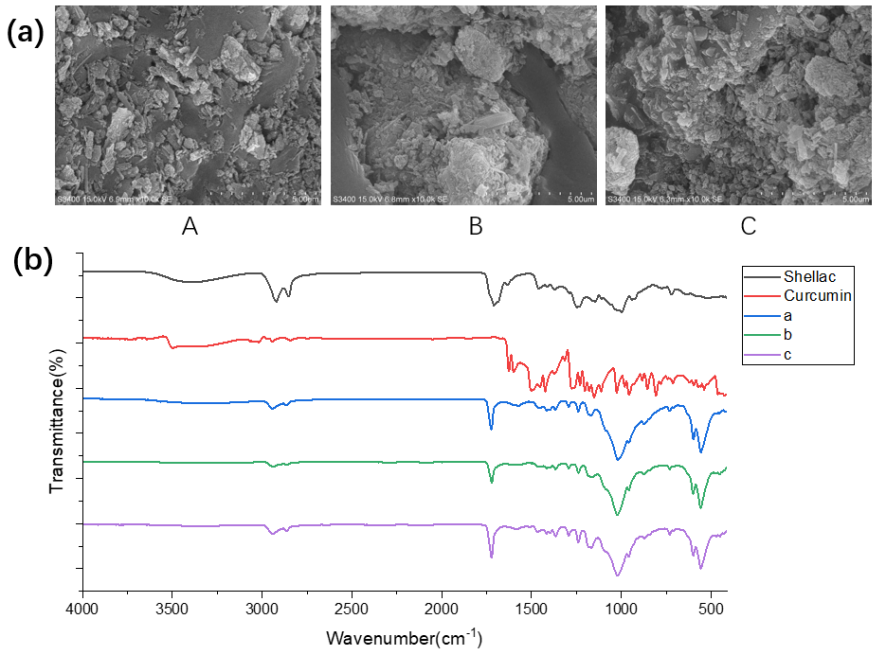

Figure 2. (a) SEM results of scaffolds. (b) FTIR spectra of shellac, curcumin and scaffolds of three groups.

surface is PCL, and the rough and irregular blocks are TCP and HA. The particle sizes of β-TCP and HA are less than 500 nm, while some of the particles are larger than 1 μm, because particles tend to aggregate to reduce surface energy. Shellac, as an adhesive, aggregates particles into larger particles after being added to the scaffold, thus showing less PCL in SEM images. FTIR spectra of the three scaffolds showed no significant difference. The addition amount of shellac and curcumin was small and did not significantly affect the curve of the scaffold. It also indicated that the addition of the two natural materials had no effect on the effective inorganic composition of osteogenesis in the blank scaffold.

3.2. Antibacterial Properties

The antibacterial properties of shellac mixed with curcumin are shown in **Figure 3**. There was no significant difference in colony area after 24 h compared with the blank group when curcumin was co-cultured with staphylococcus aureus. But with the addition of shellac, the antibacterial ability of the material was significantly improved. The average colony area calculated by ImageJ decreased from 36.2 cm^2 in the blank group to 19.7 cm^2, and the area decreased by 45.6%, while this proportion was only 15.2% in the control group. It can be seen that the combination of shellac and curcumin can significantly improve the antibacterial activity of curcumin.

3.3. Biocompatibility Test

Studies have shown that low concentrations of shellac (10 μM/mL) did not affect cell viability, but an increased concentration in shellac from 10 μM to 100 μM

resulted in an increased cell mortality from 8.5% to 30.5% [8]. This trend is also found in the CCK-8 results shown in **Figure 4(b)**. At the concentration of 2 μg/mL, the absorbance value of CCK-8 was only 12.9% of that of the blank group. However, 0.1 μg/mL shellac had no significant effect on cell proliferation. Through the concentration standard curve, the shellac concentration in the scaffold extract of group B was calculated to be 0.116 μg/mL. The results of cell living and death staining on the third day showed that shellac and shellac/curcumin scaffolds maintained good cell survival rates compared with blank scaffolds. As

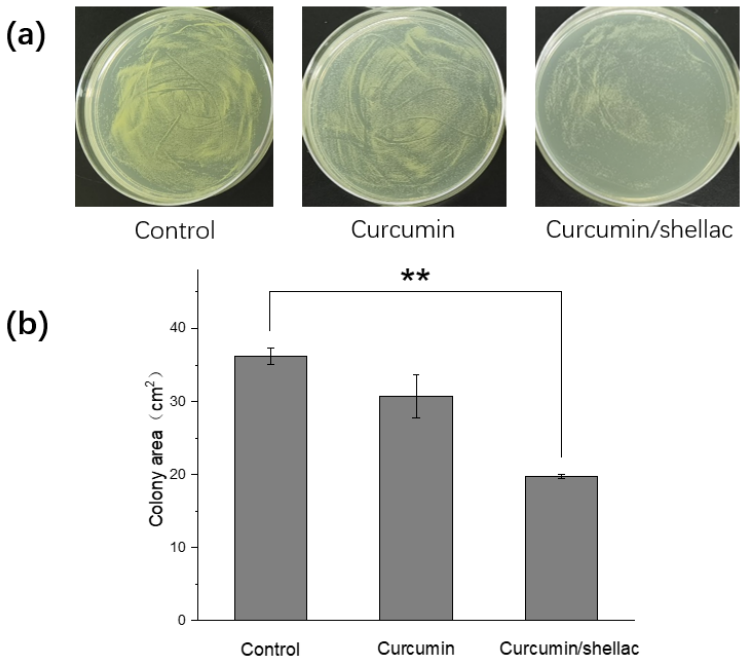

Figure 3. (a) Antibacterial properties of shellac and curcumin. (b) Comparison of colony area (**: significant difference, $P < 0.01$).

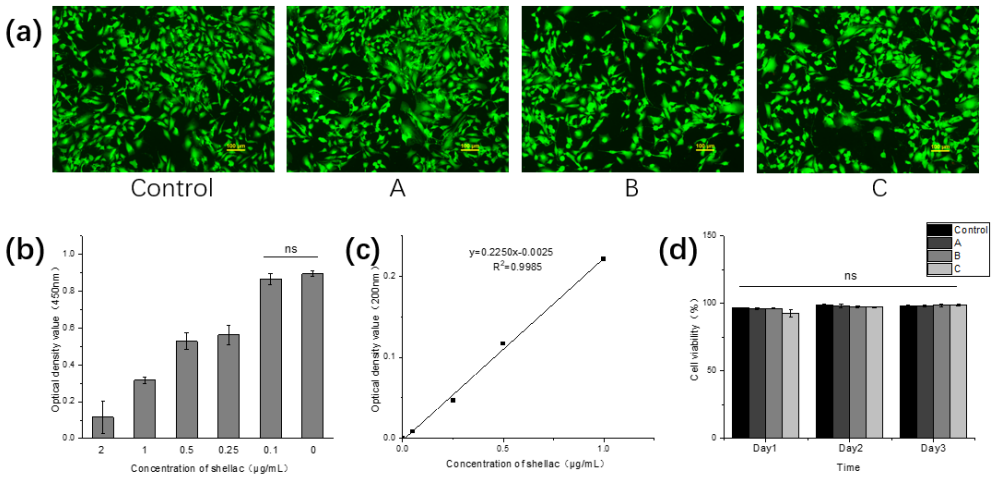

Figure 4. (a) Live/dead staining results of C2C12 cells cultured in extract. (b) CCK-8 results of C2C12 cells co-cultured with shellac. (c) Standard curve for shellac concentration. (d) Survival rate results of three days (ns: no significant difference, $P > 0.05$).

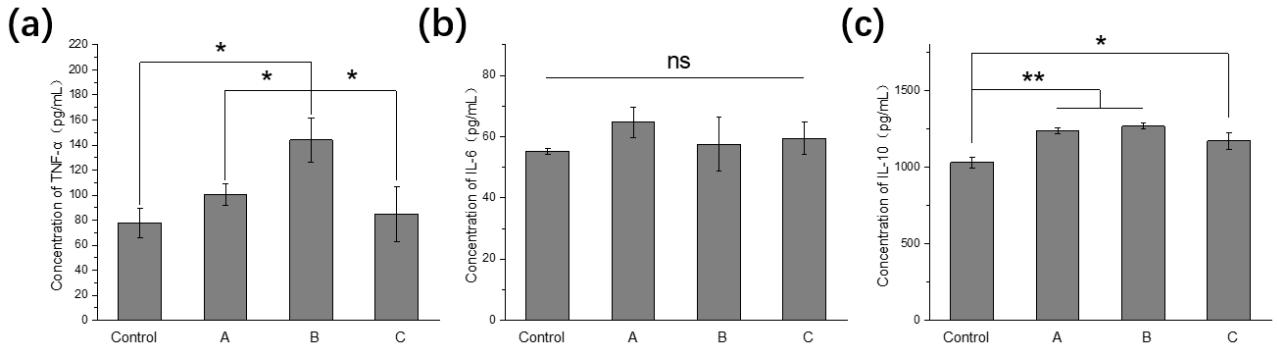

Figure 5. The concentrations of (a) TNF-α (b) IL-6 (c) IL-10 in culture medium were measured by ELISA kit after co-culture of scaffolds in groups A, B and C with THP-1 cells (ns: no significant difference, $P < 0.01$; *: significant difference, $P < 0.05$; **: significant difference, $P < 0.01$).

shown in **Figure 4(d)**, the cell survival rate remained at a high level for three days. No significant differences were found between the three groups, indicating that the addition of 1% (wt/wt) shellac and 1‰ (wt/wt) curcumin had no negative effect on cell survival.

3.4. Cytokine Assay

TNF-α and IL-6 were pro-inflammatory cytokines, while IL-10 was anti-inflammatory cytokines. There was no significant difference in IL-6 secretion level of THP-1 macrophages under the influence of the three scaffolds (**Figure 5(b)**). The level of TNF-α induced by group B was slightly higher than that in other groups, but returned to a normal level with the addition of curcumin. The IL-10 secretion levels of the three groups were significantly higher than that of the blank group, indicating that HA or hydroxyapatite and other inorganic components in the scaffold had a positive effect, while shellac and curcumin had no significant effect on it.

4. Conclusion

In this study, bone scaffolds of 80% inorganic composition incorporated with natural antibacterial compounds Shellac and curcumin were fabricated by LT-3DP. The results show that Shellac and curcumin significantly improved the antibacterial ability of the scaffolds, while maintaining good biocompatibility *in vitro* by controlling the incorporation ratio of shellac. At the same time, the scaffolds reported in this study did not cause an obvious inflammatory response, and were beneficial to increase the secretion level of IL-10 in the osteogenic microenvironment. Therefore, the multifunctional bone scaffold has great potential in implant application.

Conflicts of Interest

The authors declare no conflicts of interest regarding the publication of this paper.

References

[1] Hangge, P., Pershad, Y., Witting, A.A., Albadawi, H. and Oklu, R. (2018) Three-Dimensional (3D) Printing and Its Applications for Aortic Diseases. *Cardiovascular Diagnosis and Therapy*, **8**, S19-S25. https://doi.org/10.21037/cdt.2017.10.02

[2] Li, G., Dong, J., Cao, Z., Wang, J., Cao, D., Zhang, X., *et al.* (2021) Application of Low-Dose CT to the Creation of 3D-Printed Kidney and Perinephric Tissue Models for Laparoscopic Nephrectomy. *Cancer Medicine*, **10**, 3077-3084. https://doi.org/10.1002/cam4.3851

[3] Yu, W., Sun, X., Meng, H., Sun, B., Chen, P., Liu, X., *et al.* (2017) 3D Printed Porous Ceramic Scaffolds for Bone Tissue Engineering: A Review. *Biomaterials Science*, **5**, 1690-1698. https://doi.org/10.1039/C7BM00315C

[4] Lin, S.J., LeGeros, R.Z., Rohanizadeh, R., Mijares, D. and LeGeros, J.P. (2003) Biphasic Calcium Phosphate (BCP) Bioceramics: Preparation and Properties. In: Ben-Nissan, B., Sher, D. and Walsh, W., Eds., *Key Engineering Materials*, Vol. 240-242, 473-476. https://doi.org/10.4028/www.scientific.net/KEM.240-242.473

[5] Owen, G.R., Dard, M. and Larjava, H. (2018) Hydoxyapatite/Beta-Tricalcium Phosphate Biphasic Ceramics as Regenerative Material for the Repair of Complex Bone Defects. *Journal of Biomedical Materials Research Part B-Applied Biomaterials*, **106**, 2493-2512. https://doi.org/10.1002/jbm.b.34049

[6] Shuai, C., Yuan, X., Yang, W., Peng, S., Qian, G. and Zhao, Z. (2021) Synthesis of a Mace-Like Cellulose Nanocrystal@Ag Nanosystem via *In-Situ* Growth for Antibacterial Activities of Poly-L-lactide Scaffold. *Carbohydrate Polymers,* **262**. https://doi.org/10.1016/j.carbpol.2021.117937

[7] Zhou, K., Dong, C.F., Zhang, X.L., Shi, L., Chen, Z.C., Xu, Y.L. and Cai, H. (2015) Preparation and Characterization of Nanosilver-Doped Porous Hydroxyapatite Scaffolds. *Ceramics International*, **41**, 1671-1676. https://doi.org/10.1016/j.ceramint.2014.09.108

[8] Chang, G.H., Azar, D.A., Lyle, C., Chitalia, V.C., Shazly, T. and Kolachalama, V.B. (2019) Intrinsic Coating Morphology Modulates Acute Drug Transfer in Drug-Coated Balloon Therapy. *Scientific Reports*, **9**. https://doi.org/10.1038/s41598-019-43095-9